Manufacturing Letters 32 (2022) 28–31

Contents lists available at ScienceDirect

Manufacturing Letters

journal homepage: www.elsevier.com/locate/mfglet

Rapid and accurate prediction of temperature evolution in wire plus arc additive manufacturing using feedforward neural network

Van Thao Le [a], Hai Dang Nguyen [b], Manh Cuong Bui [a], Thinh Quy Duc Pham [b,c], Hong Thai Le [b,c], Van Xuan Tran [b], Hoang Son Tran [d,*]

[a] Le Quy Don Technical University, Hanoi, Viet Nam
[b] Institute of Development Strategies, Thu Dau Mot University, Binh Duong, Viet Nam
[c] IMSIA, CNRS, EDF, CEA, ENSTA Paris, Institut Polytechnique de Paris, 828 Boulevard des Maréchaux, 91762 Palaiseau, France
[d] Urban and Environmental Engineering, Materials and Solid Mechanics, University of Liège, Quartier Polytech 1, Allée de la Découverte 9 (B52), B-4000 Liège, Belgium

ARTICLE INFO

Article history:
Received 31 October 2021
Received in revised form 29 January 2022
Accepted 12 February 2022
Available online 22 February 2022

Keywords:
Wire plus arc additive manufacturing
Thermal cycle
Finite element
Feedforward neural network
Surrogate model

ABSTRACT

This article proposes an approach based on a feedforward neural network (FFNN-SM) and computational simulations to rapidly predict thermal cycles in multi-layer single-bead walls fabricated during wire arc additive manufacturing (WAAM). First, a finite element (FE)-based model for thermal simulation in the WAAMed part was developed. Second, a FFNN-SM was trained and validated using the data generated from thermal simulations with different heat input levels (Q). The results reveal that the developed FFNN-SM enables a accurate prediction of the temperature evolution with a global R2 value higher than 98% and within only 40 s.

1. Introduction

Wire plus arc additive manufacturing (WAAM) which uses an arc source and a metallic wire to depose layers of metals, is becoming the most suitable AM technology for producing large-size parts [1]. This technique has many advantages, such as an elevated deposition rate, flexible building volume, high material deposition efficiency, and low cost of equipment investment [2]. However, one of the most important issues related to WAAM is the high heat accumulation and complex thermal evolution during the deposition, which strongly affects the microstructures and mechanical properties of the as-built components [3]. These effects are generally investigated using experimental and numerical methods. However, due to the high experimental costs and extensive computation times in simulations, only a limited number of experimental tests and simulations have been conducted, while the interaction of process parameters in WAAM is complex [4].

To overcome the challenges mentioned above, recently, surrogate models (SM) based on machining learning techniques have been developed to quickly predict the thermal history in AM processes. For instance, Mozaffar et al. [5] and Pham et al. [6] built SMs for predicting the thermal history in directed energy deposition (DED) based on recurrent neural network (RNN) and artificial neural network (ANN). Roy et al. [7] also proposed an ANN-based SM for predicting the thermal temperature evolution in fused filament fabrication (FFF). The SM was trained and validated using the thermal data generated from the thermal simulation model. These authors demonstrated that the developed SM has a high prediction performance and low computational cost.

To the best of the authors' knowledge, there is not yet an SM for predicting the thermal history in the WAAM process. Inspired by previous works [5–8], we developed an FFNN-SM to rapidly predict the temperature evolution of any point in the part manufactured with different levels of heat input (Q). The developed model can be used for real-time monitoring and optimization of the WAAM process.

2. Methodology

Fig. 1 depicts the principle of the WAAM process considered in this study and the steps for developing an FFNN-SM to predict the thermal evolution in a WAAMed thin wall.

The WAAM process uses a gas metal arc welding (GMAW) source (Fig. 1a). The wall was built by depositing six layers from

* Corresponding author.
E-mail address: hstran@uliege.be (H.S. Tran).

https://doi.org/10.1016/j.mfglet.2022.02.003

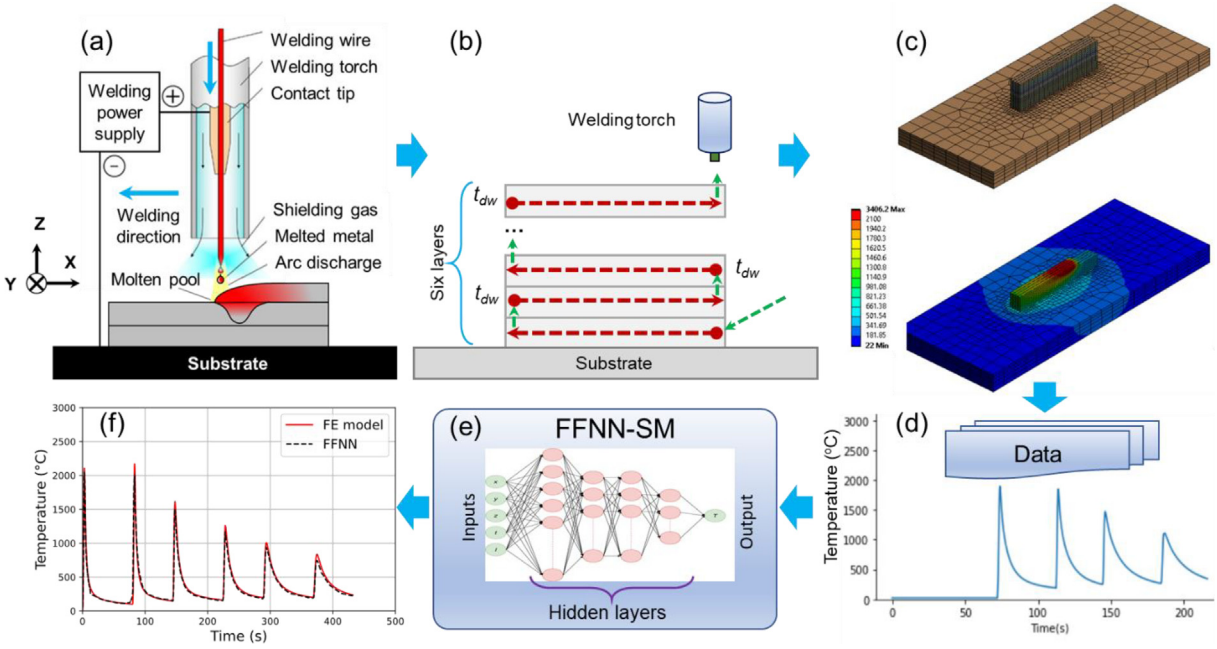

Fig. 1. (a) Schema of the GMAW-AM process, (b) deposition path for building the thin wall, (c) thermal simulation based on the FE method, (d) data generation, (e) FFNN-SM training and validation, and (f) evaluation of the accuracy of FFNN-SM.

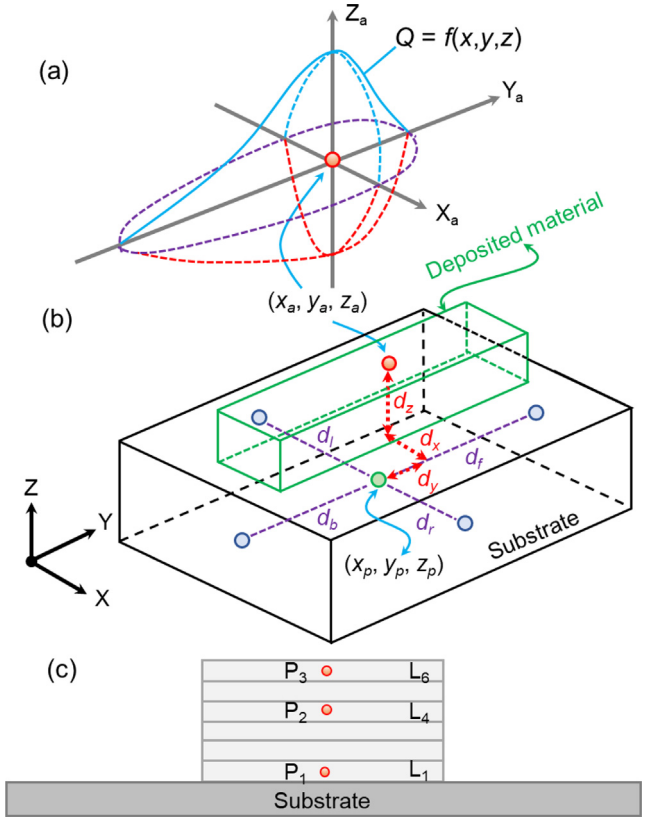

Fig. 2. (a) Goldak heat source model, (b) describing the input features of FFNN-SM, and (c) the points used to compare the thermal temperature cycles.

an SS316L substrate with a size of 200 × 80 × 10 mm and an SS316L wire, and using the zig-zag deposition method (Fig. 1b).

To develop the FFNN-SM, a finite element (FE)-based model for thermal simulation in the WAAM of a thin wall was first developed (Fig. 1c). The thermophysical properties of SS316L reported in [9], and Goldak's heat source model (Fig. 2a) [10] were chosen for the numerical simulations. The thermal simulations of the WAAM process were conducted using ANSYS software.

In this study, the FFNN-SM architecture was obtained using a trial-and-error approach. The model has four hidden layers, and the number of neurons is 70, 35, 35, and 18 for the first, second, third, and fourth-hidden layer, respectively. The model output is the temperature T at each mesh point (Fig. 1c), and the model input $\boldsymbol{q}$ is composed of five basic parameters, including the mesh point coordinates (x_p, y_p, z_p), time t, and heat input Q (Fig. 2b). In addition, to improve the performance of the FFNN-SM, other additional features, including the coordinates of the arc source – i.e., the coordinates of the Goldak heat source model origin (x_a, y_a, z_a), the distances from the mesh point to the arc source in x, y, and z-directions (d_x, d_y, d_z), and the distance from the mesh point to the side faces of the substrate (d_l, d_r, d_f, d_b), as explained in [7] and in Fig. 2b. Based on a trial-and-error method and the SHapley Additive exPlanation (SHAP) method [11], the following inputs were finally chosen for the model, $\boldsymbol{q}$ = {x_p, y_p, z_p, t, Q, x_a, z_a, d_a, and d_f}, because of their essential contributions to the prediction.

The data used to train and validate the FFNN-SM were generated from two simulations with two heat input levels, that is Q = 288 and 432 J/mm, while the travel speed was constant. For each simulation, there are 26,777,520 mesh points. Therefore, the data points used to train and validate the FFNN-SM are 53555040. The model accuracy was evaluated with Q = 331, 346, and 389 J/mm. The metric used to evaluate the model accuracy is R^2, Eq. (1), where N_v is the size of the testing dataset, $T_{FFNN\text{-}SM}$ is the predicted temperature, T_{FE} is the simulation temperature, and $\overline{T}$ is the mean simulation temperature. In particular, the temperature evolution obtained by the FFNN-SM and the simulation was compared in detail at three points {P_1, P_2, and P_3} – the middle points of the layers L_1, L_4, and L_6, respectively (Fig. 2c).

$$R^2 = 1 - \frac{\sum_{j=1}^{N_v}\left(T_{FFNN-SM}{}^{(j)} - T_{FE}^{(j)}\right)^2}{\sum_{j=1}^{N_v}\left(\overline{T} - T_{FE}^{(j)}\right)^2} \quad (1)$$

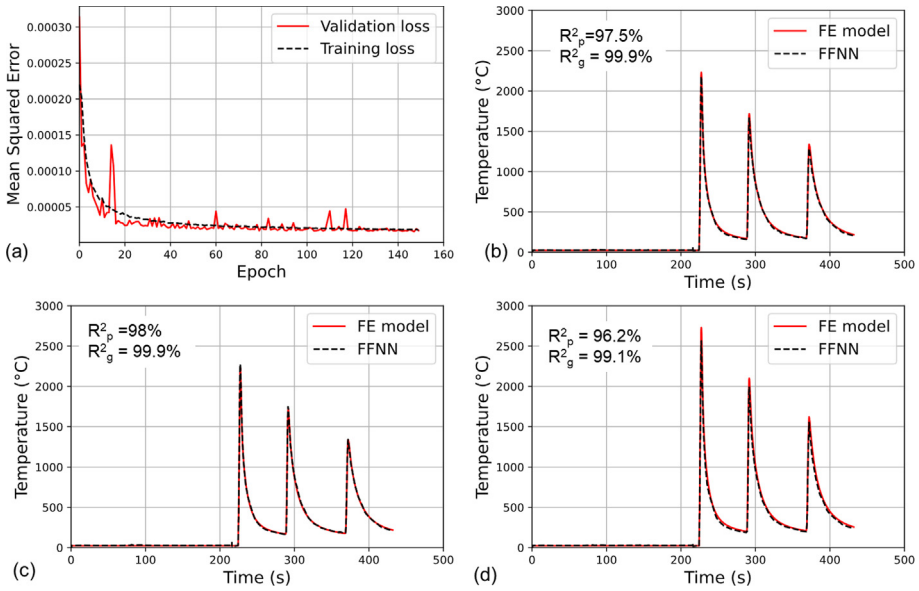

Fig. 3. (a) Training and validation losses of FFNN-SM and the comparison between the simulated and predicted temperature evolution at the point P_2: (b) Q_1 = 331, (c) Q_2 = 346, and (d) Q_3 = 389 J/mm.

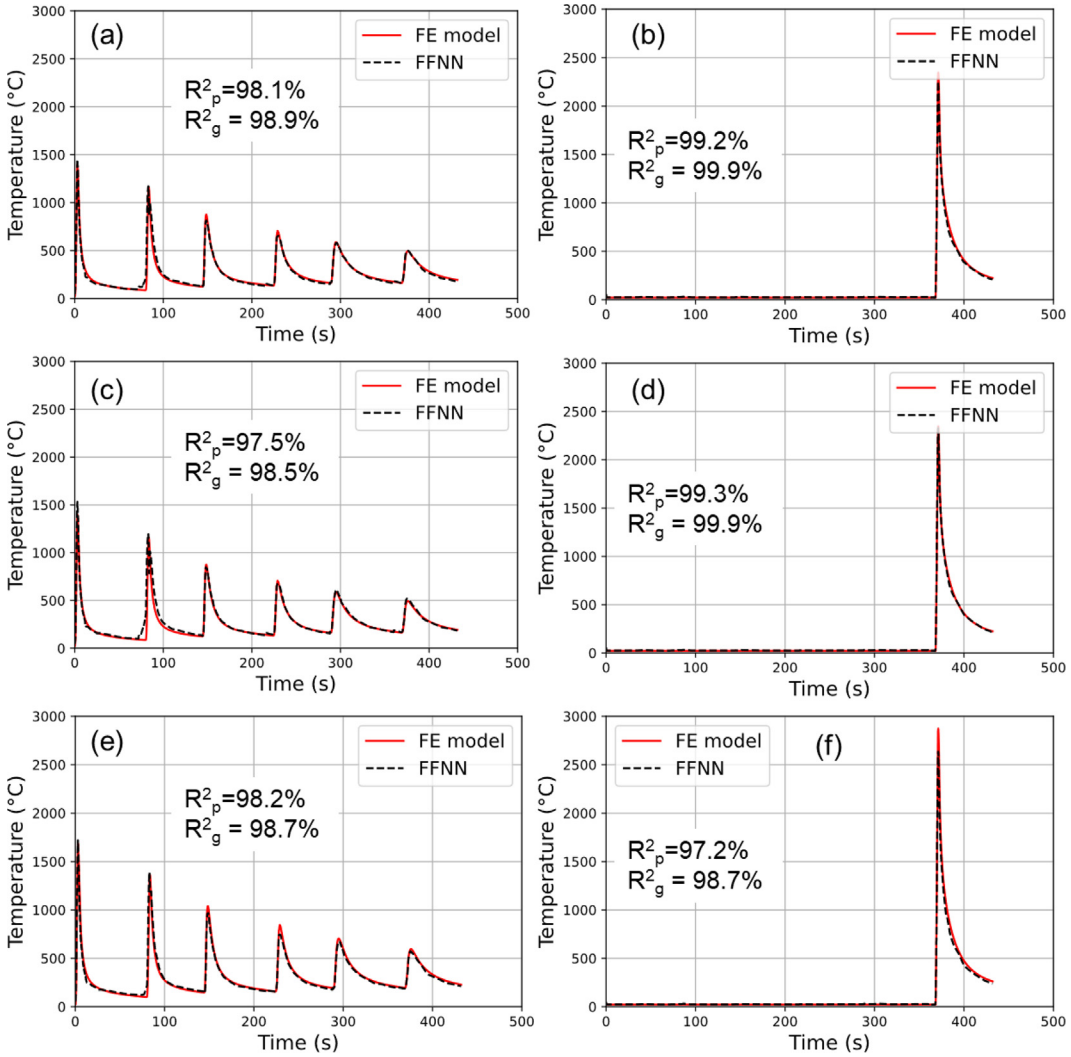

Fig. 4. Comparison between the simulated and predicted temperature evolution at the points P1 (a, c, e) and P3 (b, d, f) in the cases of (a, b) Q_1 = 331, (c, d) Q_2 = 346, and (e, f) Q_3 = 389 J/mm.

3. Results and discussion

As shown in Fig. 3a, it can be seen that the FFNN-SM converges relatively rapidly after approximately 150 epochs because no further decrease in the cross-validation training loss is observed. This indicates that there is neither overfitting nor underfitting of the model and confirms the model reliability. The global R^2 (R_g^2) and the R^2 of the temperature peak (R_p^2) in all test cases reached 99.9% and higher than 96%, respectively (Fig. 3b-d), demonstrating the good accuracy of the FFNN-SM prediction capability.

Fig. 4 shows the comparison between the temperature evolutions obtained from FFNN-SM and the FM simulation for two points: P_1 and P_3 in three cases (Q_1, Q_2, and Q_3). It can be seen that the FFNN-SM can accurately describe the thermal cycles of these points in the sense that both the temperature peaks and cooling cycles are precisely reproduced. The values of R_g^2 and R_p^2 calculated for these points are consistently higher than 98% and 97%, respectively.

In terms of the computational time, the time required to train the FFNN-SM is approximately 3.5 h using GPU computing. However, after training, the FFNN-SM only takes 40 s to predict the whole temperature field, compared to 4.5 h for the FE model. This means the FFNN-SM enables considerably reducing computational time and making it possible to perform a large amount of data in a relatively short time. Therefore, when a large number of simulations need to be performed to predict thermal cycles in the WAAM process, the FFNN-SM with high accuracy can be used to replace the FE model.

4. Conclusions

This work developed an FFNN-SM to estimate the temperature field with different heat inputs in the WAAM process of thin walls using the simulation data. It is shown that the surrogate model can accurately estimate the thermal field evolutions of any mesh point with a global R^2 value higher than 98%. Both temperature peaks during deposition and cooling cycles of the points can be captured perfectly by the surrogate model. Without considering the data generation and training, the execution time is only 40 s, compared to about 4.5 h needed for a FE simulation. In future works, it is expected that this method can be applied to other problems relevant to the AM fields, such as predicting thermal-induced stresses and deformation during the WAAM process or the residual distortion of final parts.

Declaration of Competing Interest

The authors declare that they have no known competing financial interests or personal relationships that could have appeared to influence the work reported in this paper.

Acknowledgments

This work was funded by Vingroup and supported by Vingroup Innovation Foundation (VINIF) under project code VINIF.2020.DA15.

References

[1] Williams SW, Martina F, Addison AC, Ding J, Pardal G, Colegrove P. Wire + arc additive manufacturing. Mater. Sci. Technol. 2016;32(7):641–7. https://doi.org/10.1179/1743284715Y.0000000073.
[2] Ding D, Pan Z, Cuiuri D, Li H. Wire-feed additive manufacturing of metal components: technologies, developments and future interests. Int. J. Adv. Manuf. Technol. 2015;81(1-4):465–81. https://doi.org/10.1007/s00170-015-7077-3.
[3] Jafari D, Vaneker THJ, Gibson I. Wire and arc additive manufacturing: opportunities and challenges to control the quality and accuracy of manufactured parts. Mater. Des. 2021;202:109471. https://doi.org/10.1016/j.matdes.2021.109471.
[4] Xie X, Bennett J, Saha S, Lu Ye, Cao J, Liu WK, et al. Mechanistic data-driven prediction of as-built mechanical properties in metal additive manufacturing. Npj Comput. Mater. 2021;7(1). https://doi.org/10.1038/s41524-021-00555-z.
[5] Mozaffar M, Paul A, Al-Bahrani R, Wolff S, Choudhary A, Agrawal A, et al. Data-driven prediction of the high-dimensional thermal history in directed energy deposition processes via recurrent neural networks. Manuf. Lett. 2018;18:35–9. https://doi.org/10.1016/j.mfglet.2018.10.002.
[6] Pham QDT, Hoang TV, Pham QT, Huynh TP, Tran VX, Fetni S, et al. Data-driven prediction of temperature evolution in metallic additive manufacturing process. Esaform 2021;2021(13):1–10. https://doi.org/10.25518/esaform21.2599.
[7] Roy M, Wodo O. Data-driven modeling of thermal history in additive manufacturing. Addit Manuf 2020;32:101017. https://doi.org/10.1016/j.addma.2019.101017.
[8] Fetni S, Pham QDT, Tran VX, Duchêne L, Tran HS, Habraken AM. Thermal field prediction in DED manufacturing process using Artificial Neural Network. ESAFORM 2021;2021(13):1–10. https://doi.org/10.25518/esaform21.2812.
[9] Lee SH. CMT-based wire arc additive manufacturing using 316L stainless steel: effect of heat accumulation on the multi-layer deposits. Metals (Basel) 2020;10:278. https://doi.org/10.3390/met10020278.
[10] Goldak J, Chakravarti A, Bibby M. A new finite element model for welding heat sources. Metall Trans B 1984;15(2):299–305. https://doi.org/10.1007/BF02667333.
[11] Lundberg SM, Lee S-I. A Unified Approach to Interpreting Model Predictions. Proc. 31st Int. Conf. Neural Inf. Process. Syst. 2017:4768–77.